A&A, 708, A147 (2026)
https://doi.org/10.1051/0004-6361/202658971

Astronomy & Astrophysics

A data-driven estimate of the protosolar helium mass fraction

G. Buldgen[1,⋆], M. Kunitomo[2], A. Noels[1], T. Guillot[3], R. Scuflaire[1], and N. Grevesse[1,4]

[1] STAR Institute, Université de Liège, Liège, Belgium
[2] Department of Physics, Kurume University, 67 Asahimachi, Kurume, Fukuoka 830-0011, Japan
[3] Université Côte d'Azur, Observatoire de la Côte d'Azur, CNRS, Laboratoire Lagrange, Bd de l'Observatoire, CS 34229, 06304 Nice cedex 4, France
[4] Centre Spatial de Liège, Université de Liège, Angleur-Liège, Belgium

Received 15 January 2026 / Accepted 2 March 2026

ABSTRACT

Context. The protosolar helium mass fraction is a fundamental ingredient of solar, planetary models and enrichment laws used to model stellar populations. However, the assumed values often rely on simplifying descriptions of the transport of chemicals in solar models. Furthermore, they are based on the inferred helium mass fraction in the solar convective envelope, which is itself sensitive to uncertainties in the equation of state of the solar material.
Aims. We aim to update the reference protosolar helium abundance by taking into account the effects of macroscopic mixing at the base of the convective zone and using more recent determinations of the helium mass fraction in the convective envelope.
Methods. We combined results from our own inversions of the composition of the solar envelope with spectroscopic abundances, as well as values in the literature, to provide a robust interval of the current helium mass fraction in the convective zone. We combined this measurement with solar models taking into account light element depletion to provide an updated protosolar helium abundance.
Results. We show that macroscopic mixing at the base of the convective envelope of the Sun cannot be neglected to infer the protosolar helium abundance. We demonstrate that as soon as this effect is included, the protosolar helium abundance is significantly reduced and that lithium and beryllium depletion can be used to calibrate this effect over the solar evolution. We find a revised interval of a primordial helium mass fraction of 0.27575 ± 0.00315 slightly lower than previous estimates when combining our latest estimate of the surface helium mass fraction and spectroscopic abundances. We find that the effects of macroscopic mixing are partially compensated by an increase in the inferred solar helium mass fraction in recent studies, but also derive more precise estimates based on various reference works in the literature. If the usual surface helium mass fraction is used, the primordial helium mass fraction drops to 0.2669 ± 0.00415 as a result of the inclusion of macroscopic mixing. The dominant source of uncertainty on this value is found to be the surface helium abundance inferred from helioseismic constraints and, more specifically, the impact on the equation of state of the solar material on this inference result.

Key words. Sun: abundances – Sun: fundamental parameters – Sun: helioseismology – Sun: oscillations

1. Introduction

The protosolar helium abundance, denoted Y_P, is an important ingredient of planetary models, particularly when simulating the evolution of the giant planets of the Solar System (see e.g. Guillot et al. 1997; Nettelmann et al. 2015; Mankovich et al. 2016; Howard et al. 2024; Nettelmann et al. 2024; Nettelmann & Fortney 2025). Thanks to helioseismology, we are able to estimate the current helium mass fraction in the convective zone (CZ) of the Sun, denoted Y_{CZ} (Vorontsov et al. 1991; Basu & Antia 1995; Richard et al. 1998; Di Mauro et al. 2002; Basu & Antia 2004; Vorontsov et al. 2013, 2014; Buldgen et al. 2024a). Each of these studies found a slightly different (though often overlapping at 1σ) value. The most commonly cited is $Y_{CZ} = 0.24875 \pm 0.0035$ from Basu & Antia (2004), which is compatible to the value reported by Richard et al. (1998) of $Y_{CZ} = 0.2480 \pm 0.0020$. However, these results remain bound to the accuracy of the equation of state of the solar material, and, in practice, the reported values and associated uncertainties may significantly differ (see Sect. 4), as can be seen from the results from Di Mauro et al. (2002) $Y_{CZ} = 0.2539 \pm 0.0005$ when using the OPAL equation of state (Rogers et al. 1996; Rogers & Nayfonov 2002) and $Y_{CZ} = 0.2457 \pm 0.0005$ when using the magnetohydrodynamic (MHD) equation of state (Hummer & Mihalas 1988; Mihalas et al. 1988; Daeppen et al. 1988; Mihalas et al. 1990). Later studies by Vorontsov et al. (2013) and Vorontsov et al. (2014), combining both OPAL and SAHA-S (Gryaznov et al. 2004, 2006, 2013; Baturin et al. 2013) equations of state, report lower precisions of $Y_{CZ} = 0.2475 \pm 0.0075$ and $Y_{CZ} = 0.2525 \pm 0.0075$, which are dominated by uncertainties in the equation of state.

The main source of discrepancies between all these studies is the equation of state of the solar plasma, thus motivating continued improvements of the equation of state used in solar and stellar models to achieve higher precision (Antia & Basu 1994; Baturin & Däppen 2003; Trampedach et al. 2006; Baturin et al. 2025; Trampedach & Däppen 2025). All the results above are very consistent with each other, but their respective precision vary significantly, with more recent estimate by Vorontsov et al. (2013) and Vorontsov et al. (2014) being less precise by a factor of two over the usual value taken from Basu & Antia (2004). As we explain below, such a large uncertainty has a direct impact on the protosolar helium mass fraction. To infer the protosolar

⋆ Corresponding author: gbuldgen@uliege.be

helium mass fraction, it is necessary to link the current surface helium mass fraction to the protosolar one by assuming and/or simulating the evolution of helium during the life of the Sun. The best way to do this is by computing solar models and analysing the changes in surface composition and its link with the current surface composition of the Sun. Therefore, this relation intrinsically includes a model-dependent dimension through the hypotheses made on the physical ingredients of the solar models, the most straightforward one being mixing prescriptions for chemicals.

Early works by Serenelli & Basu (2010) estimated the protosolar helium abundance from the analysis of a large number of standard solar models (SSMs). They also included some early models simulating turbulence at the base of the solar convective envelope in their work. This work, however, only considered one estimate of the surface helium abundance (Basu & Antia 1995, 2004), which has since been revised using different equations of state (Vorontsov et al. 2013, 2014; Buldgen et al. 2024a) and did not include the depletion of lithium and beryllium in the study of the evolution of the surface helium abundance. However, they considered a 20% uncertainty in microscopic diffusion and related the primordial helium abundance to the surface one using scaling laws from Bahcall (1989). The uncertainties on the treatment of microscopic diffusion have since improved thanks to the full treatment of the effects and extensive comparisons of solar models (Turcotte et al. 1998; Deal et al. 2025). We also refer the reader to Michaud et al. (2015) for a more in-depth discussion on microscopic diffusion.

In this work, we took advantage of the recent determination of lithium (A(Li) = 0.96 ± 0.05) (Wang et al. 2021) and beryllium (A(Be) = 1.21 ± 0.05) (Amarsi et al. 2024), which are key tracers of the efficiency of the turbulent mixing at the base of the convective zone (BCZ), as these light elements are depleted when compared to meteoritic values, A(Li) = 3.27 ± 0.03 and A(Be) = 1.31 ± 0.04 (Lodders 2021). In previous works (Buldgen et al. 2023, 2025a), we showed that including a calibrated mixing efficiency on both elements strongly impacted the initial helium abundance of solar models as well as the conclusions one could draw when comparing solar models to helioseismic constraints. In Deal et al. (2025), we showed that these results were also obtained with various stellar evolution codes and calibration procedures. Using various ingredients that affect the helium mass fraction evolution (opacities, overshooting, nuclear rates) within the same numerical framework, we aim to provide a robust estimation of the primordial helium abundance.

We start in Sect. 2 by discussing the various physical hypotheses that may influence the primordial helium value, separating what concerns the transport of chemicals and other ingredients that will indirectly influence the evolution of the helium mass fraction in the envelope. From this analysis, we can draw an estimate of the difference between the primordial and current envelope helium mass fraction in Sect. 2.2 and finally an estimate of the primordial helium mass fraction in Sect. 4. We conclude by discussing additional improvements to solar models that may help us further increase the precision of this estimate in the coming years.

2. Solar models

In this section we present the properties of the solar models computed with the Liège Stellar Evolution Code (Scuflaire et al. 2008), which we will use to infer the primordial solar helium abundance, Y_P. We used the AAG21 solar abundances (Asplund et al. 2021), the OPAL (Iglesias & Rogers 1996) and LANL/OPLIB (Colgan et al. 2016) opacities, the mixing-length formalism of convection following Cox & Giuli (1968), the SAHA-S equation of state (version 7), and the NACRE II nuclear reaction rates (Xu et al. 2013). Our models include the Thoul et al. (1994) formalism of diffusion, including the Paquette et al. (1986) screening coefficients, and consider partial ionisation of the chemical elements. Turbulence was treated following Proffitt & Michaud (1991) as in Buldgen et al. (2025a). However, given the similarities found in Buldgen et al. (2025a) and Deal et al. (2025) for other analytical expressions of the empirical turbulent diffusion coefficient, this does not constitute a limitation on the conclusions we draw on turbulence at the BCZ.

The main properties of our solar models are summarised in Table 1, considering first only the effects of turbulent diffusion at the BCZ, and Table 2, where we considered a change of reference opacities, overshooting, and turbulent diffusion. The results for the models considering both the effects of overshooting and turbulent diffusion over a large range of parameters are provided in Table A.1. We used the following naming convention: D_Y^X implies the inclusion of an additional diffusion coefficient in cm^2/s of the following form, as in Proffitt & Michaud (1991):

$$D_Y^X = Y\left(\frac{\rho_{\mathrm{BCZ}}}{\rho}\right)^X, \tag{1}$$

with ρ_{BCZ} being the density at the BCZ position and ρ the local density. X and Y are the free parameters in the coefficient that have to be calibrated (usually on light element depletion).

The addition of the suffix 'LANL' implies the use of the Los Alamos/OPLIB opacities (Colgan et al. 2016), while 'Ov Z' implies the inclusion of overshooting at the BCZ, over a fraction of the local pressure scale height defined by Z, enforcing instantaneous mixing of chemicals and an adiabatic temperature gradient in the overshooting region.

One can already see that directly inferring Y_P from calibrated solar evolutionary models is not feasible given the interdependences between the physical ingredients of solar models (see e.g. Christensen-Dalsgaard 2021, and refs therein for a recent review). For example, changing the opacity tables in solar models will directly affect Y_P as a change of opacity in the core of the Sun needs to be compensated such that the solar-calibrated model reproduces the solar luminosity at the solar age (see e.g. Buldgen et al. 2019, for a discussion for a wide range of ingredients of solar models). However, we can already see a crucial element of the evolution of the chemical composition of the solar envelope. Namely, looking at the slope of the values of Y_{CZ}, two effects stand out. First, the intensity of turbulence at the BCZ strongly affects the efficiency of settling; for example, in the SSM, the value of Y_{CZ} is significantly lower. Second, the physical conditions at the BCZ (e.g. its position, the temperature gradients, etc.) will also slightly affect the helium depletion over time, although on a much smaller scale. Indeed, microscopic diffusion effects are a combination of temperature, pressure, and chemical composition contributions (e.g. Turcotte et al. 1998; Baturin et al. 2006). We illustrate this by plotting the diffusion velocity of helium for three solar models of our sample in Fig. 1.

As can be seen, the presence of turbulence directly affects the diffusion velocity at the BCZ. The differences between the SSM and the model including turbulence from Proffitt & Michaud (1991) go as high as 30%, explaining the observed differences in Y_{CZ} at the age of the Sun. This effect is visible even for the lower intensity of turbulent diffusion, even when overshooting

Table 1. Global parameters of the solar evolutionary models including turbulent diffusion.

Name	$(r/R)_{BCZ}$	Y_{CZ}	Y_P	$A(Li)$ (dex)	$A(Be)$ (dex)
SSM	0.7263	0.2371	0.2653	3.28	1.36
D^2_{1500}	0.7250	0.2469	0.2650	1.87	1.22
D^2_{1700}	0.7251	0.2471	0.2649	1.78	1.20
D^2_{2000}	0.7252	0.2473	0.2648	1.66	1.18
D^2_{2500}	0.7254	0.2477	0.2646	1.46	1.13
D^2_{3500}	0.7256	0.2483	0.2643	1.11	1.05
D^2_{4000}	0.7257	0.2486	0.2642	0.94	1.01
D^2_{4500}	0.7258	0.2488	0.2642	0.78	0.98
D^2_{5500}	0.7260	0.2491	0.2641	0.48	0.91
D^3_{6500}	0.7255	0.2481	0.2644	0.97	1.15
D^3_{6700}	0.7255	0.2481	0.2644	0.94	1.14
D^3_{7500}	0.7256	0.2483	0.2643	0.80	1.12

Table 2. Global parameters of the solar evolutionary models using the OPLIB opacities, including overshooting and turbulent diffusion.

Name	$(r/R)_{BCZ}$	Y_{CZ}	Y_P	$A(Li)$ (dex)	$A(Be)$ (dex)
LANL Ov 0.17 D^1_{750}	0.7122	0.2383	0.2557	1.48	1.17
LANL Ov 0.17 D^1_{850}	0.7123	0.2386	0.2556	1.41	1.14
LANL Ov 0.17 D^2_{1250}	0.7120	0.2383	0.2556	1.38	1.22
LANL Ov 0.1 D^2_{1150}	0.7176	0.2380	0.2558	1.83	1.24
LANL Ov 0.15 D^2_{1450}	0.7137	0.2385	0.2555	1.41	1.20
LANL Ov 0.12 D^2_{1750}	0.7163	0.2387	0.2554	1.45	1.18
LANL Ov 0.22 D^2_{1250}	0.7079	0.2385	0.2555	1.01	1.21
LANL Ov 0.25 D^2_{1150}	0.7053	0.2385	0.2555	0.81	1.21

is considered, and already well before the models reproduce the lithium and/or beryllium depletion. This implies that such a reduction of the efficiency of microscopic diffusion remains relevant if the uncertainties of the current lithium and beryllium abundances were underestimated.

As it impacts the transport of all elements during the evolution of the Sun, turbulent diffusion at the BCZ has a direct impact on the solar calibration procedure. Indeed, a calibrated solar model must reproduce the solar radius, luminosity, and surface metallicity at the age of the Sun. Due to the effect of turbulence, the evolution of the metals is also impacted, meaning that the initial conditions of the solar calibration are affected by the presence of extra mixing or by variations of the BCZ position. We illustrate this well-known effect in Fig. 2 with the evolution of the surface metallicity, which has been reported in numerous publications (see e.g. Richard et al. 1996; Gabriel 1997; Brun et al. 2002; Christensen-Dalsgaard et al. 2018; Buldgen et al. 2025a). The fact that the BCZ position can be precisely located using helioseismology strongly constrains the allowed variations and, therefore, the impact on the chemical evolution of the position of the convective envelope.

2.1. Impact of light element depletion on the helium mass fraction

Reproducing the observed depletion of lithium and beryllium is a crucial component of the chemical evolution of the Sun and Sun-like stars. While the exact underlying physical mechanism is still unknown, as recent candidates (Eggenberger et al. 2022) were unable to reproduce lithium and beryllium simultaneously (Buldgen et al. 2025a), it is clear that the observed depletion is due to additional mixing occurring at the BCZ. Previous works (Schlattl & Weiss 1999; Zhang et al. 2019) have shown that the depletion of lithium can be reproduced by overshooting, but this process does not induce any beryllium depletion (Kunitomo et al. 2025); it is thus at odds with observations (Amarsi et al. 2024). Results in Eggenberger et al. (2022) also showed that overshooting induced too high a depletion of lithium in young solar twins in open clusters, implying that its impact should be limited. Additionally, Buldgen et al. (2025b) showed that overshooting cannot simultaneously reproduce the properties of the CZ – such as the BCZ position and the height of the entropy plateau in the CZ – while an opacity increase at the BCZ can. These results tend to favour recent hydrodynamical simulations advocating for a limited extent of overshooting at the BCZ. In this context, solar models must reproduce the BCZ position, the entropy plateau height, and the lithium and beryllium depletions simultaneously. Such models can only be produced by assuming ad hoc modifications to the opacity profile and/or additional phenomena or modifications to the physical ingredients (see e.g., amongst others, Guzik et al. 2006; Christensen-Dalsgaard et al. 2009; Serenelli et al. 2009; Ayukov & Baturin 2011, 2017; Buldgen et al. 2019; Zhang et al. 2019; Kunitomo & Guillot 2021; Kunitomo et al. 2022).

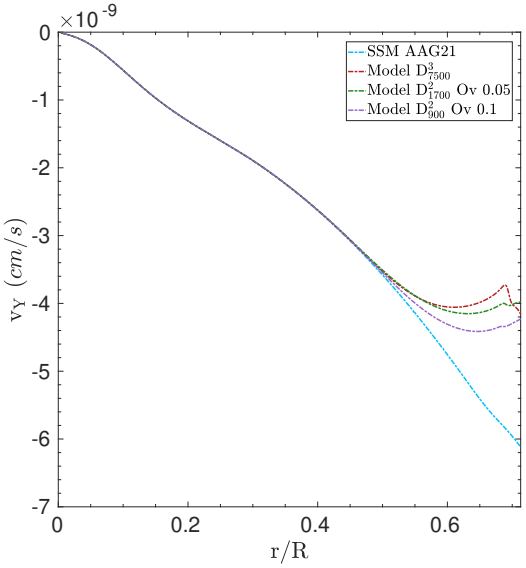

Fig. 1. Diffusion velocity of helium for as a function of normalised radius in the radiative zone of solar models (a SSM in light blue and models including macroscopic mixing and/or overshooting at the BCZ in red, green, and purple).

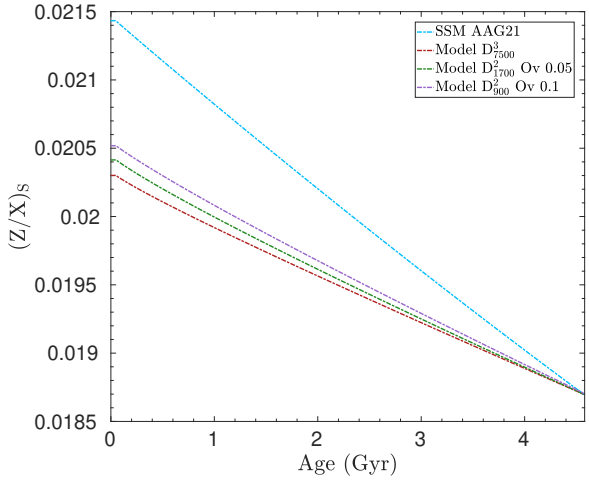

Fig. 2. Evolution of surface metallicity of calibrated solar models, $(Z/X)_S$, as a function of time (a SSM in light blue and models including macroscopic mixing and/or overshooting at the BCZ in red, green, and purple). The assumed final metallicity at the solar age is that of Asplund et al. (2021).

Even considering the lithium and beryllium depletions as relatively loose constraints, the overall variation of Y_{CZ}, presented in Fig. 3, remains quite similar for a fixed set of physical ingredients. The differences compared to those of an SSM (shown here in red and denoted SSM AAG21) are striking, with a lower Y_P found in models including turbulence.

In Fig. 4 we illustrate the corresponding depletion of lithium and beryllium as a function of time in these models. As mentioned above, we did not consider the lithium and beryllium depletion to be strong constraints and allowed for models in stark disagreement with observations. Nevertheless, even by considering models with significantly lower depletion of light elements then the ones observed, the effect of turbulence of Y_{CZ} and Y_P was immediate. This is a direct consequence of the impact of turbulence on the diffusion velocities, meaning that the snapshot

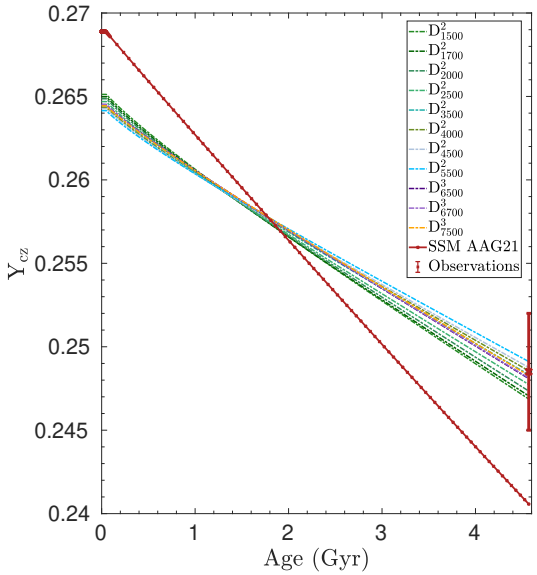

Fig. 3. Evolution of helium mass fraction in the convective envelope as a function of time for the models of Table 1. The observed value (red cross) is taken as that of Basu & Antia (2004).

illustrated at the solar age in Fig. 1, where the efficient settling is already damped, happens at much lower efficiencies of turbulent mixing at the BCZ and throughout the evolution of solar models. This demonstrates that the protosolar helium abundance cannot be inferred without considering the impact of turbulence at the BCZ, at it would induce a significant overestimation of its value.

2.2. Importance of the physical ingredients of solar models

As mentioned before, physical ingredients of solar models may play a crucial role. Radiative opacities at high temperatures have a significant impact on Y_P, with the latest OPLIB opacities leading to a lower value. This change is a direct consequence of a variation of the central temperature of the Sun induced by the intrinsically lower OPLIB opacities in this regime. A similar effect was observed in Ayukov & Baturin (2017) when changing the efficiency of nuclear reactions, or the opacity at high temperatures (see Christensen-Dalsgaard 2021, and refs therein for a detailed discussion). This effect is illustrated in the left panel of Fig. 5, where we can see the evolution of Y_{CZ}.

In addition to the effect of a change in opacity, we considered the impact of overshooting at the BCZ. As shown in various publications, adding overshooting leads to an enhanced depletion of lithium, particularly during the pre-main-sequence phase. While this is at odds with young solar twins in open clusters, we still considered the combined impact of overshooting and turbulent diffusion at the BCZ to investigate its potential impact on the evolution of Y_{CZ}. If we compare the right panel of Fig. 5 to Fig. 3, we can see that the impact is negligible. In other words, the evolution of the BCZ position under the effect of overshooting has no influence on the depletion of helium, it is solely dominated by turbulence at the BCZ.

In Figs. A.1 and A.2, we also illustrate the evolution of the surface lithium and beryllium abundances as a function of time for the models of Tables A.1 and 2. While the models cover a wide range of final values for both lithium and beryllium, their evolution of Y_{CZ} remains similar, implying that the dominant factor is purely the presence of turbulent diffusion at the BCZ. This

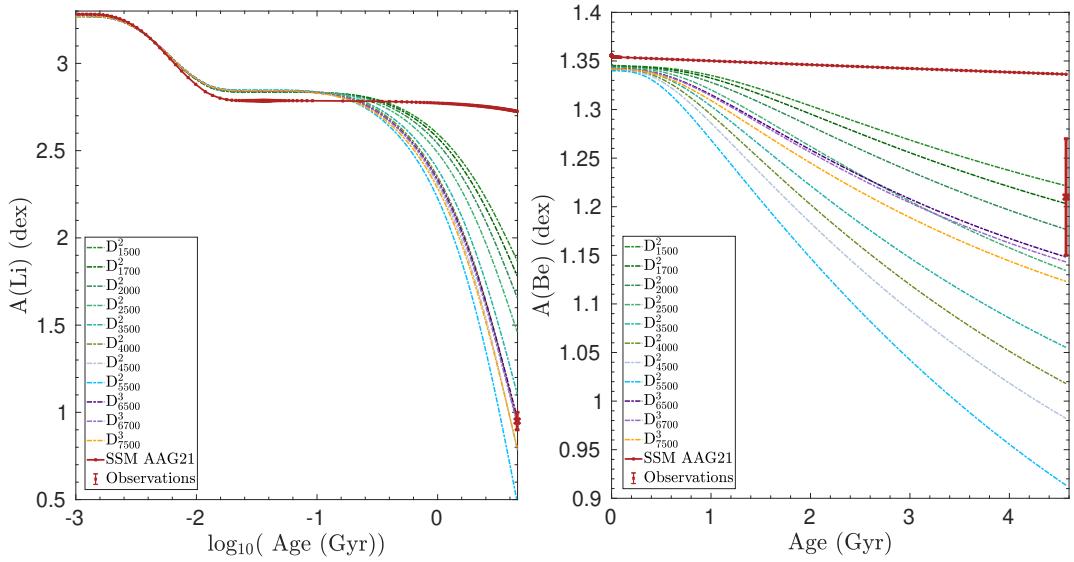

Fig. 4. Left panel: Evolution of surface lithium abundance as a function of age (in log scale) for the models of Table 1. The observed value is taken from Wang et al. (2021). Right panel: Evolution of surface beryllium abundance as a function of age (in log scale) for the models of Table 1. The observed value is taken from Amarsi et al. (2024).

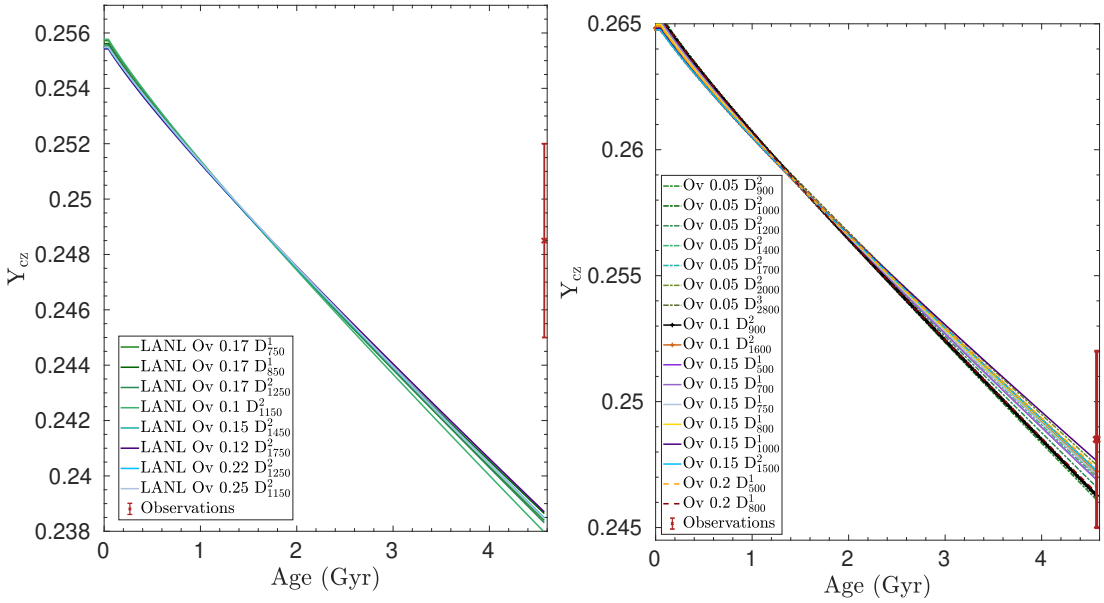

Fig. 5. Left panel: Evolution of helium mass fraction in the convective envelope as a function of time for the models of Table 2. The observed value (red cross) is taken as that of Basu & Antia (2004). Right panel: Evolution of helium mass fraction in the convective envelope as a function of time for the models of Table A.1.

remains true for a wide range of overshooting values and under the effect of a change of reference opacity tables. Indeed, the only effect of changing the OPAL opacity tables with the OPLIB opacity tables is a vertical shift of Y_P, which is a simple consequence of the initial conditions of the calibration procedure that requires the calibrated model to reproduce the solar luminosity at the solar age (among other constraints). A direct consequence of the left panel of Fig. 5 is that non-standard models reproducing both lithium and beryllium depletion using the OPLIB opacity tables will not be able to reproduce the Y_{CZ} values inferred from helioseismology when using the AAG21 abundances[1]. The problem is less stringent if a higher solar metallicity is considered (e.g. using the MB22 abundances from Magg et al. 2022); however, as shown in Buldgen et al. (2023) and Buldgen et al. (2024b), a strong disagreement remains with neutrino fluxes, confirming that uncertainties on radiative opacities might not only be an issue at temperatures of the BCZ.

[1] This issue has already been discussed extensively in Buldgen et al. (2019) for a wide variety of physical ingredients.

3. Evolution of the helium mass fraction in the convective envelope

As shown in Sect. 2.2, the absolute value of helium abundance in the CZ may vary depending on numerous physical ingredients, but the BCZ position itself has little impact. As already

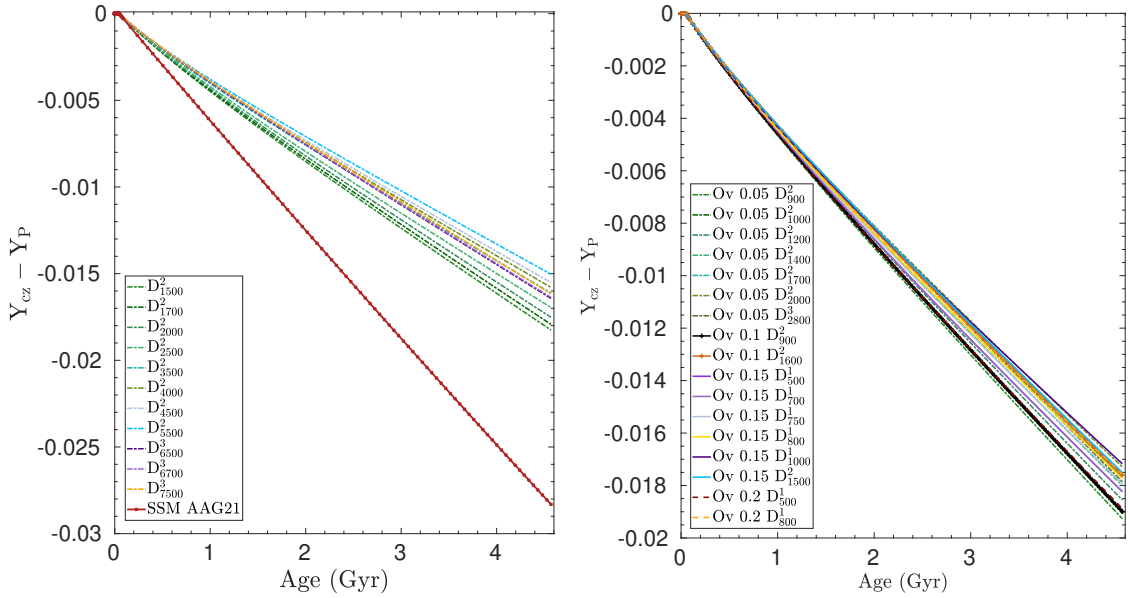

Fig. 6. Left panel: Evolution of difference between the protosolar and surface abundance of helium (Y_{CZ}-Y_P) as a function of time for the models of Table 1. Right panel: Same as the left panel but for the models of Table 2.

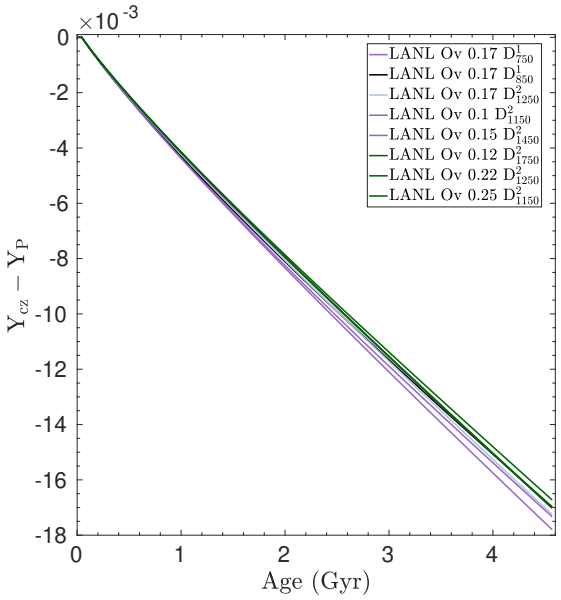

Fig. 7. Evolution of difference between the protosolar and surface abundance of helium (Y_{CZ}-Y_P) as a function of time for the models of Table 2.

demonstrated in previous works (Serenelli & Basu 2010), the only factors determining the value of Y_{CZ} are the initial conditions (thus Y_P) and the efficiency with which helium settles from the BCZ. In this respect, we emphasise the crucial role of turbulent diffusion at the BCZ in the previous sections. We highlight that it would significantly affect the settling of helium even without considering the current lithium and beryllium abundances as strong constraints in the calibration.

To further illustrate this point, in Figs. 6 and 7 we plot the differences between the initial and primordial helium abundance, Y_{CZ}-Y_P, as a function of time. In all cases, the variation is quite similar and much smaller than the one obtained with an SSM, which is illustrated in the left panel of Fig. 6. The same trend is always obtained, whatever the physical ingredients; the more efficient the turbulent diffusion at the BCZ, the lower the efficiency of settling and the lower the lithium value and beryllium at the age of the Sun. An important point is that the effect of the opacities has been completely erased, as the observed differences, Y_{CZ}-Y_P, for models using OPLIB opacities or OPAL opacities remain well within the same range. This confirms that we can directly infer Y_P from the knowledge of Y_{CZ} and the efficiency of the transport at the BCZ quantified through Y_{CZ}-Y_P at the solar age.

From a quantitative point of view, the value Y_{CZ}-Y_P for the SSM is −0.02831, which is very similar to what was found in Serenelli & Basu (2010). As soon as turbulent diffusion is included, considering our entire set of models, this value drops within an interval between −0.01523 and −0.1921. If we consider the lithium and beryllium depletion as strong constraints, this interval further decreases to values between −0.01750 and −0.01888. This means that using an SSM instead of models taking into account light element depletion induces an overestimation of Y_{CZ}-Y_P by about 40%, significantly biasing the estimated protosolar helium abundance.

4. Protosolar helium estimated using the helioseismology of the solar envelope

In this section, we describe how we combined spectroscopic constraints, helioseismic constraints, and the inferred properties of Y_{CZ}-Y_P to recover an updated value of Y_P. To do this, we made use of the Γ_1 inversions of Buldgen et al. (2024a), and more specifically the inferences in the higher part of the convective envelope, from which the helium abundance can be estimated. In Fig. 8, we show an example of an χ^2 map used in this work, on which we overlaid the surface area covered when assuming a value of $Z/X = 0.0187 \pm 0.0009$ in agreement with AAG21. In practice, and as shown in Serenelli & Basu (2010), the assumed Z/X has little impact on the inferred Y_{CZ} using helioseismic inversions. It may be neglected to first order, but one should keep in mind that some signatures of the partial ionisation of metals

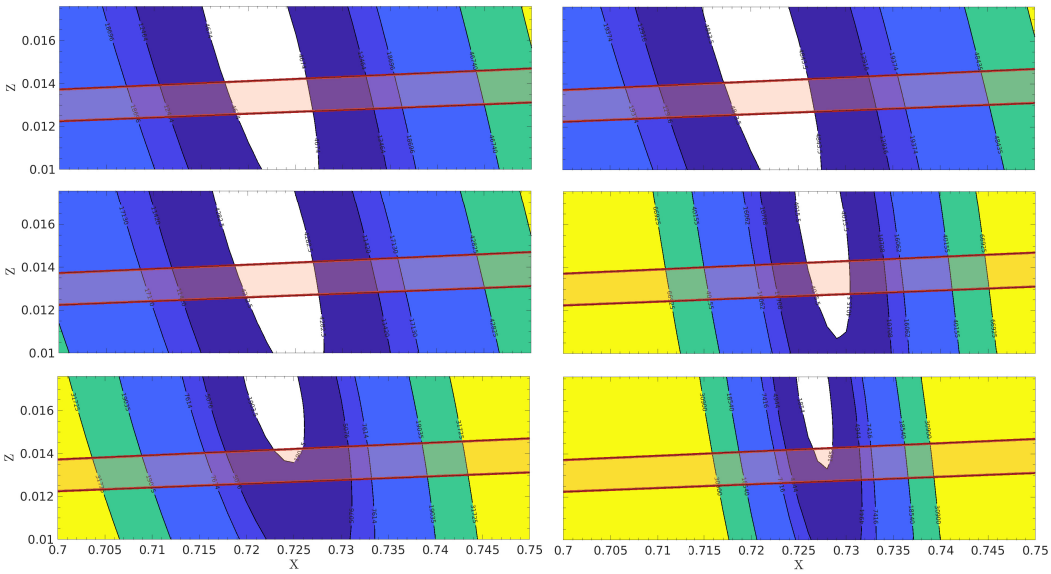

Fig. 8. χ^2 maps used in Buldgen et al. (2024a) to determine the value of the hydrogen mass fraction as a function of the metal mass fraction in the solar convective envelope. The properties of the models are summarised in their Table 3. The red band shows the range of values compatible with the AAG21 $(Z/X)_S$ value.

Table 3. Helium mass fraction inferred from various groups in the literature.

Reference	Y_{CZ}	Equation of state
Richard et al. (1998)	0.2480 ± 0.0020	OPAL
Di Mauro et al. (2002)	0.2457 ± 0.0005	MHD
Di Mauro et al. (2002)	0.2539 ± 0.0005	OPAL
Basu & Antia (2004)	0.24875 ± 0.0035	OPAL
Vorontsov et al. (2013)	0.2475 ± 0.0075	OPAL and SAHA-S
Vorontsov et al. (2014)	0.2525 ± 0.0075	OPAL and SAHA-S
This work	0.2575 ± 0.0025	FreeEOS and SAHA-S

in the Γ_1 profile are also present at the temperatures where we infer the Y_{CZ} value (see e.g. Baturin et al. 2022, for an illustration of the contributions of metals to the Γ_1 profile), inducing a small interdependence between the inferred Y_{CZ} and Z_{CZ} (the CZ's metal mass fraction) that can be seen in Vorontsov et al. (2013) and Vorontsov et al. (2014).

In order to perform a rudimentary global analysis, we summarise some Y_{CZ} inference results from the literature in Table 3. These values span over three decades of observations, with different instruments, datasets, methods, and equations of state. Overall, the range found is not too different between the various works. However, we can note that the equation of state largely dominates the uncertainty budget in the inference. This underlines the much needed improvements of the solar equation of state as mentioned in Baturin et al. (2025), Trampedach & Däppen (2025).

From our previous work, (Buldgen et al. 2024a) combined with Asplund et al. (2021), we find the following interval for Y_{CZ} from our χ^2 maps: 0.255−0.26. It is in line with the higher values of the results of Vorontsov et al. (2013) and Vorontsov et al. (2014). The main contributor to the uncertainty is again the equation of state, as we considered both SAHA-S (v3 and v7) and FreeEOS (Irwin 2012) for these inferences. It appears that this interval encompasses most of the ones found in Table 3. If we now combine these values to the Y_{CZ}-Y_P differences found in previous sections, we obtain the following result for each Y_{CZ}, assuming strong constraints on lithium and beryllium depletion:

- For Richard et al. (1998): $Y_P = 0.26619 \pm 0.00269$.
- For Di Mauro et al. (2002) (MHD): $Y_P = 0.26385 \pm 0.00115$.
- For Di Mauro et al. (2002) (OPAL): $Y_P = 0.27205 \pm 0.00115$.
- For Basu & Antia (2004): $Y_P = 0.2669 \pm 0.00415$.
- For Vorontsov et al. (2013): $Y_P = 0.26565 \pm 0.00815$.
- For Vorontsov et al. (2014): $Y_P = 0.27065 \pm 0.00815$.
- For this work: $Y_P = 0.27565 \pm 0.00315$.

A very conservative estimate for Y_P would fall between 0.2552 and 0.2792, considering the lowest (highest) estimates of Y_{CZ}, namely 0.24 and 0.26, combined with the lowest (highest) estimate of Y_{CZ}-Y_P, namely −0.01523 and −0.1921. If we consider only the most recent works and considering the depletion of lithium and beryllium as strong constraints to be achieved by solar models, this interval is reduced to $[0.2725, 0.2789]$. Our value is slightly lower, yet consistent with the interval found by Serenelli & Basu (2010) $[0.272, 0.284]$, but for entirely different reasons. In our case, the Y_{CZ} is intrinsically higher than theirs due to the Y_{CZ} intervals found in the latest analyses, whereas our depletion of helium over time is lower as a result of the inhibition of settling by turbulence at the BCZ.

In fact, had we considered their Y_{CZ} and our conservative Y_{CZ}-Y_P values, we would have found Y_P to be within $[0.2605, 0.271]$. This is even lower than their value estimated from non-SSMs which in their case did not include light ele-

ment depletion. In all cases, the uncertainties on the Y_{CZ} value largely dominate the total budget, with uncertainties on the equation of state dominating the uncertainties on Y_{CZ} itself (see e.g. Kosovichev et al. 1992, for an early discussion).

It should also be underlined that the various references provided in Table 3 used different techniques to infer Y_{CZ}, as well as different datasets from different instruments. This may give rise to small systematic differences as noted in Basu & Antia (2004) or Buldgen et al. (2024a), the authors of which used revised Michelson Doppler Imager data. Another tedious point is that of surface effect corrections. Apart from the works of Vorontsov et al. (2013) and Vorontsov et al. (2014), all other methods used the individual frequencies directly and thus had to rely on empirical corrections for the surface effects, following, for example, Rabello-Soares et al. (1999) or using a newly derived expression for high-degree modes (Di Mauro et al. 2002). It should also be noted that the differences between Vorontsov et al. (2013) and Vorontsov et al. (2014) stem from different techniques, as the former used two approaches based on the phase shift of frequencies, while the latter used group velocities of the solar acoustic modes. In this context, the uncertainties provided on Y_{CZ} are directly related to the ones of the inversion technique, and thus in the case of a given technique mentioned above (such as the SOLA technique in Buldgen et al. 2024a), they only include the propagation of the observational error bars on the frequencies and not other sources of errors.

Therefore, an improvement of Y_P would also require us to improve the inference of Y_{CZ} and carry out a detailed meta-analysis of the overall procedure. In order words, to consistently analyse the impact of various helioseismic datasets, various inference techniques, and equations of state used to determine the value of Y_{CZ}, as well as various transport prescriptions (using, e.g. various stellar evolution codes) on the inferred value of Y_P. Such an analysis is beyond the scope of this work and would only be conclusive if the various equations of state available to solar modellers were to be tested within this framework, using Markov chain Monte Carlo or bootstrap techniques to provide robust uncertainties on the inferred Y_{CZ} value.

5. Conclusion

In this study, we analysed the dependences of the inference of the protosolar helium mass fraction, Y_P, in detail, with the aim of determining an updated value. We show that using SSMs leads to a significant overestimation (by about 40%) of the depletion of helium from the CZ during the solar evolution when compared to solar models reproducing light element depletion. This result is independent of the opacity tables used or of the inclusion of overshooting at the BCZ. We show that the lithium and beryllium abundances at the solar age could serve as efficient calibrators of the efficiency of mixing at the BCZ during the main-sequence evolution of the Sun. Using these constraints, we carried out a meta-analysis of all the values in the literature and inferred an updated interval for Y_P. A very conservative estimate would be $Y_P = 0.2672 \pm 0.012$.

When only considering the values for Y_{CZ} from Buldgen et al. (2024a) and lithium and beryllium as strong constraints, we find $Y_P = 0.2757 \pm 0.0032$. This demonstrates the importance of considering the constraints on chemical mixing at the BCZ, as it significantly increases the precision of the inferred Y_P value.

This value remains consistent with that of Serenelli & Basu (2010) of $Y_P = 0.278 \pm 0.006$, but this is due to a compensation effect as the Y_{CZ} values inferred in recent works is higher than the one from (Basu & Antia 1995) used in Serenelli & Basu (2010). Taking their value of Y_{CZ} and remaining conservative on the effects of lithium and beryllium depletion, we find $Y_P = 0.2669 \pm 0.00415$. This difference underlines the importance of taking into account macroscopic mixing at BCZ, as one cannot assume that SSMs provide an accurate representation of the chemical evolution of the solar convective envelope as they only include microscopic diffusion. The quoted value of $Y_P = 0.2669 \pm 0.00415$ is perfectly consistent with the value reported in the work of Kunitomo et al. (2025) that used an extended calibration scheme including protosolar accretion and the Y_{CZ} value of Basu & Antia (2004) and the OPAL equation of state to describe the solar plasma. It is also noteworthy that protosolar accretion does not affect the inferred value of Y_P unless the helium mass fraction of the accreted material is significantly different from the protosolar one (such an hypothesis was made in Zhang et al. 2019).

Improving the precision of the inference of Y_P using solar models first requires us to improve the uncertainties on the Y_{CZ} value itself. This requires further improvement of the accuracy of the equation of state of the solar plasma, as it is the main source of uncertainty in the helioseismic inference of Y_{CZ}. The second factor influencing the Y_{CZ} is the depiction of the outer convective envelope and the so-called surface effect. Limiting their impact by using averaged 3D hydrodynamical simulations instead of grey atmosphere models would bring us closer to resolving the issue. The third limiting factor in the precision of Y_P is the transport of chemicals at the BCZ. While the physical nature of the macroscopic mixing at the BCZ is unknown, its overall efficiency and impact can still be empirically calibrated using the observed depletion of lithium and beryllium. In this respect, an improved precision on the inference of the current beryllium abundance in the solar photosphere would directly impact our uncertainty on Y_P. Indeed, the beryllium depletion is an important anchoring point for the efficiency of mixing during the main sequence, while lithium is partially burned during the pre-main sequence.

The above statement does not imply that improvements to the way the transport of chemicals at the BCZ itself is modelled would not significantly increase the precision of the inferred value of Y_P. A better understanding of the transport of chemicals in the Sun is in any case paramount to improving solar models in general and our inference of stellar ages in light of the requirements of the PLATO mission (Rauer et al. 2025). However, it is likely that the lithium and beryllium depletion will remain crucial observational constraints to confront models with improved transport of chemicals.

Acknowledgements. We thank the referee for their careful reading of the manuscript. GB acknowledges fundings from the Fonds National de la Recherche Scientifique (FNRS) as a postdoctoral researcher. M.K. was supported by JSPS KAKENHI Grant Nos. JP24K00654 and JP24K07099.

References

Amarsi, A. M., Ogneva, D., Buldgen, G., et al. 2024, A&A, 690, A128
Antia, H. M., & Basu, S. 1994, ApJ, 426, 801
Asplund, M., Amarsi, A. M., & Grevesse, N. 2021, A&A, 653, A141
Ayukov, S. V., & Baturin, V. A. 2011, J. Phys. Conf. Ser., 271, 012033
Ayukov, S. V., & Baturin, V. A. 2017, Astron. Rep., 61, 901
Bahcall, J. N. 1989, Neutrino Astrophysics
Basu, S., & Antia, H. M. 1995, MNRAS, 276, 1402
Basu, S., & Antia, H. M. 2004, ApJ, 606, L85
Baturin, V. A., & Däppen, W. 2003, Astron. Rep., 47, 685
Baturin, V. A., Gorshkov, A. B., & Ayukov, S. V. 2006, Astron. Rep., 50, 1001
Baturin, V. A., Ayukov, S. V., Gryaznov, V. K., et al. 2013, ASP Conf. Ser., 479, 11

Baturin, V. A., Oreshina, A. V., Däppen, W., et al. 2022, A&A, 660, A125
Baturin, V. A., Ayukov, S. V., Oreshina, A. V., et al. 2025, Sol. Phys., 300, 3
Brun, A. S., Antia, H. M., Chitre, S. M., & Zahn, J.-P. 2002, A&A, 391, 725
Buldgen, G., Salmon, S. J. A. J., Noels, A., et al. 2019, A&A, 621, A33
Buldgen, G., Eggenberger, P., Noels, A., et al. 2023, A&A, 669, L9
Buldgen, G., Noels, A., Baturin, V. A., et al. 2024a, A&A, 681, A57
Buldgen, G., Noels, A., Scuflaire, R., et al. 2024b, A&A, 686, A108
Buldgen, G., Noels, A., Amarsi, A. M., et al. 2025a, A&A, 694, A285
Buldgen, G., Noels, A., Baturin, V. A., et al. 2025b, A&A, 700, A50
Christensen-Dalsgaard, J. 2021, Liv. Rev. Sol. Phys., 18, 2
Christensen-Dalsgaard, J., di Mauro, M. P., Houdek, G., & Pijpers, F. 2009, A&A, 494, 205
Christensen-Dalsgaard, J., Gough, D. O., & Knudstrup, E. 2018, MNRAS, 477, 3845
Colgan, J., Kilcrease, D. P., Magee, N. H., et al. 2016, ApJ, 817, 116
Cox, J. P., & Giuli, R. T. 1968, Principles of Stellar Structure (Gordon and Breach)
Daeppen, W., Mihalas, D., Hummer, D. G., & Mihalas, B. W. 1988, ApJ, 332, 261
Deal, M., Buldgen, G., Manchon, L., et al. 2025, Sol. Phys., 300, 96
Di Mauro, M. P., Christensen-Dalsgaard, J., Rabello-Soares, M. C., & Basu, S. 2002, A&A, 384, 666
Eggenberger, P., Buldgen, G., Salmon, S. J. A. J., et al. 2022, Nat. Astron., 6, 788
Gabriel, M. 1997, A&A, 327, 771
Gryaznov, V. K., Ayukov, S. V., Baturin, V. A., et al. 2004, AIP Conf. Ser., 731, 147
Gryaznov, V. K., Ayukov, S. V., Baturin, V. A., et al. 2006, J. Phys. A Math. Gen., 39, 4459
Gryaznov, V. K., Iosilevskiy, I. L., Fortov, V. E., et al. 2013, Contrib. Plasma Phys., 53, 392
Guillot, T., Gautier, D., & Hubbard, W. B. 1997, Icarus, 130, 534
Guzik, J. A., Watson, L. S., & Cox, A. N. 2006, Mem. Soc. Astron. It., 77, 389
Howard, S., Müller, S., & Helled, R. 2024, A&A, 689, A15
Hummer, D. G., & Mihalas, D. 1988, ApJ, 331, 794
Iglesias, C. A., & Rogers, F. J. 1996, ApJ, 464, 943
Irwin, A. W. 2012, Astrophysics Source Code Library [record ascl:1211.002]
Kosovichev, A. G., Christensen-Dalsgaard, J., Daeppen, W., et al. 1992, MNRAS, 259, 536
Kunitomo, M., & Guillot, T. 2021, A&A, 655, A51
Kunitomo, M., Guillot, T., & Buldgen, G. 2022, A&A, 667, L2
Kunitomo, M., Buldgen, G., & Guillot, T. 2025, A&A, 702, A167
Lodders, K. 2021, Space Sci. Rev., 217, 44
Magg, E., Bergemann, M., Serenelli, A., et al. 2022, A&A, 661, A140
Mankovich, C., Fortney, J. J., & Moore, K. L. 2016, ApJ, 832, 113
Michaud, G., Alecian, G., & Richer, J. 2015, Atomic Diffusion in Stars
Mihalas, D., Dappen, W., & Hummer, D. G. 1988, ApJ, 331, 815
Mihalas, D., Hummer, D. G., Mihalas, B. W., & Daeppen, W. 1990, ApJ, 350, 300
Nettelmann, N., & Fortney, J. J. 2025, Planet. Sci. J., 6, 98
Nettelmann, N., Fortney, J. J., Moore, K., & Mankovich, C. 2015, MNRAS, 447, 3422
Nettelmann, N., Cano Amoros, M., Tosi, N., Helled, R., & Fortney, J. J. 2024, Space Sci. Rev., 220, 56
Paquette, C., Pelletier, C., Fontaine, G., & Michaud, G. 1986, ApJS, 61, 177
Proffitt, C. R., & Michaud, G. 1991, ApJ, 380, 238
Rabello-Soares, M. C., Basu, S., & Christensen-Dalsgaard, J. 1999, MNRAS, 309, 35
Rauer, H., Aerts, C., Cabrera, J., et al. 2025, Exp. Astron., 59, 26
Richard, O., Vauclair, S., Charbonnel, C., & Dziembowski, W. A. 1996, A&A, 312, 1000
Richard, O., Dziembowski, W. A., Sienkiewicz, R., & Goode, P. R. 1998, A&A, 338, 756
Rogers, F. J., & Nayfonov, A. 2002, ApJ, 576, 1064
Rogers, F. J., Swenson, F. J., & Iglesias, C. A. 1996, ApJ, 456, 902
Schlattl, H., & Weiss, A. 1999, A&A, 347, 272
Scuflaire, R., Théado, S., Montalbán, J., et al. 2008, ApSS, 316, 83
Serenelli, A. M., & Basu, S. 2010, ApJ, 719, 865
Serenelli, A. M., Basu, S., Ferguson, J. W., & Asplund, M. 2009, ApJ, 705, L123
Thoul, A. A., Bahcall, J. N., & Loeb, A. 1994, ApJ, 421, 828
Trampedach, R., & Däppen, W. 2025, Sol. Phys., 300, 7
Trampedach, R., Däppen, W., & Baturin, V. A. 2006, ApJ, 646, 560
Turcotte, S., Richer, J., Michaud, G., Iglesias, C. A., & Rogers, F. J. 1998, ApJ, 504, 539
Vorontsov, S. V., Baturin, V. A., & Pamiatnykh, A. A. 1991, Nature, 349, 49
Vorontsov, S. V., Baturin, V. A., Ayukov, S. V., & Gryaznov, V. K. 2013, MNRAS, 430, 1636
Vorontsov, S. V., Baturin, V. A., Ayukov, S. V., & Gryaznov, V. K. 2014, MNRAS, 441, 3296
Wang, E. X., Nordlander, T., Asplund, M., et al. 2021, MNRAS, 500, 2159
Xu, Y., Takahashi, K., Goriely, S., et al. 2013, Nucl. Phys. A, 918, 61
Zhang, Q.-S., Li, Y., & Christensen-Dalsgaard, J. 2019, ApJ, 881, 103

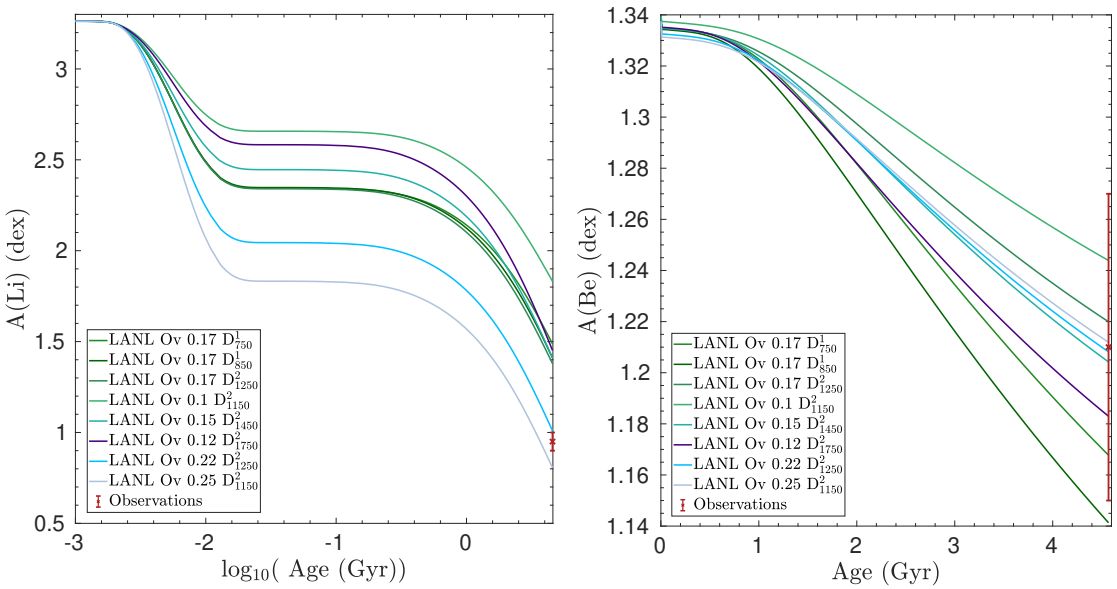

Fig. A.1. Left panel: Evolution of surface Lithium abundance as a function of age (in log scale) for the models of Table 2. The 'Observed' value is taken from Wang et al. (2021). Right panel: Evolution of the surface Beryllium abundance as a function of age (in log scale) for the models of Table 2. The "Observed" value is taken from Amarsi et al. (2024).

Appendix A: Additional table and figures

We provide in Table A.1 the fundamental parameters of our models including both overshooting and turbulent diffusive mixing at the BCZ. We illustrate in Figs. A.1 and A.2 the lithium and beryllium depletion of our models including overshooting at the BCZ and using the Los Alamos opacities instead of the OPAL opacities. The mixing efficiencies and overshooting values are varied far beyond what would be considered reasonable regarding light element depletion.

Table A.1. Global parameters of the solar evolutionary models including overshooting and turbulent diffusion.

Name	$(r/R)_{\rm BCZ}$	$Y_{\rm CZ}$	$Y_{\rm P}$	$A(Li)$ **(dex)**	$A(Be)$ **(dex)**
Ov 0.05 D^2_{900}	0.7210	0.2461	0.2653	1.93	1.27
Ov 0.05 D^2_{1000}	0.7210	0.2463	0.2652	1.88	1.26
Ov 0.05 D^2_{1200}	0.7210	0.2466	0.2650	1.78	1.24
Ov 0.05 D^2_{1500}	0.7210	0.2470	0.2649	1.63	1.21
Ov 0.05 D^2_{1700}	0.7211	0.2472	0.2648	1.54	1.19
Ov 0.05 D^2_{2000}	0.7212	0.2475	0.2647	1.41	1.16
Ov 0.05 D^3_{2800}	0.7211	0.2471	0.2648	1.48	1.25
Ov 0.1 D^2_{900}	0.7166	0.2462	0.2652	1.64	1.26
Ov 0.1 D^2_{1600}	0.7171	0.2472	0.2647	1.29	1.19
Ov 0.15 D^1_{500}	0.7126	0.2461	0.2653	1.44	1.23
Ov 0.15 D^1_{700}	0.7130	0.2469	0.2650	1.27	1.17
Ov 0.15 D^1_{1000}	0.7135	0.2477	0.2647	1.03	1.09
Ov 0.15 D^2_{1500}	0.7130	0.2473	0.2647	0.97	1.19
Ov 0.17 D^1_{750}	0.7115	0.2471	0.2649	1.06	1.16
Ov 0.17 D^1_{800}	0.7116	0.2472	0.2649	1.02	1.14
Ov 0.2 D^1_{500}	0.7086	0.2464	0.2652	1.02	1.22
Ov 0.2 D^1_{800}	0.7091	0.2473	0.2648	0.76	1.14

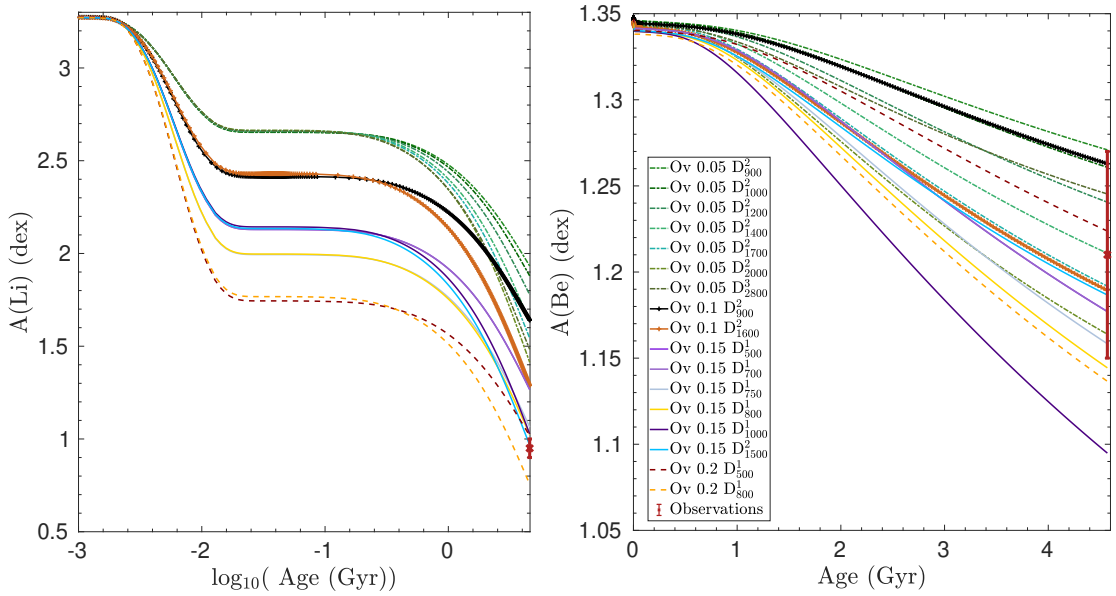

Fig. A.2. Left panel: Evolution of surface Lithium abundance as a function of age (in log scale) for the models of Table A.1. The 'Observed' value is taken from Wang et al. (2021). Right panel: Evolution of the surface Beryllium abundance as a function of age (in log scale) for the models of Table A.1. The "Observed" value is taken from Amarsi et al. (2024).